

1 General comments

2 This paper shows that a 6-year oscillation is visible in the time-varying gravity recorded by 6
3 Superconducting Gravimeters (SGs). The origin of this 6-year oscillation also seen in other
4 geophysical and geodetic time-series is still debated today. A core origin has been suggested but
5 surficial climatic events could also be responsible for that periodic oscillation. This paper completes
6 the catalog of observables containing a 6-year oscillation. It confirms that it is a global effect. They
7 then try to prove that it is of internal origin, but as discussed here after, it is not so clear, and hydrology
8 still prevails. The methods they employed are not new either, and one of their method (AR-z spectrum)
9 could even raise some criticism. There are also a few scientific flaws and worries that need to be
10 considered and corrected, in particular with respect to the published literature.

11 **Response:** We are grateful for your comments and corrections on some of the interpretations that we
12 made as well as some of the technical errors that we made, which will assist to improve the work. Our
13 replies to your comments can be found below.

14

15

16 Specific comments (individual scientific questions/issues)

17 This paper is a follower of a series of studies by Pr. Hao Ding and co-workers who support a core
18 origin for the 6-year oscillation observed in geodetic and gravimetric data, despite some evidence for
19 a more probable surficial origin by Rosat et al. (2021). The criticism can be reproduced here, since
20 hydrological loading does also contain a 6-yr oscillation contrary to what the authors claim (Fig. S5 is
21 not at the same scale as Fig.3 so it is misleading). If you do plot the FFT spectra of ERAIn or ERA5
22 (or ERA5_land) hydrological loading products, as I did, you will see a non-negligible contribution
23 around 6-year. You can also plot the time-series of SG gravity residuals with respect to hydrological
24 loading, band-pass filtered them around 6-yr, and you will see a good correlation between both time-
25 series, for most worldwide SG stations of sufficient data length, but with a time-shift for some stations.
26 You have to consider cautiously the sign of the local contribution of hydrological loading for
27 underground stations like Moxa, Membach and Strasbourg. Indeed, another group of researchers has
28 shown that the continental hydrology as well as other climatic time-series exhibit a 6-year oscillation
29 e.g. Pfeffer et al. (2022, <https://doi.org/10.5194/egusphere-2022-1032>), Cazenave et al. (2023,
30 <https://doi.org/10.5194/egusphere-2023-312>) and Pfeffer et al. (2023,

31 <http://ssrn.com/abstract=4388237>). This hydrological signal contributes to the observed 6-yr gravity
32 change and would mask any potential signal originating from the core. Consequently, as long as you
33 do not correctly deconvolve gravity data from this hydrological signal, you cannot interpret the 6-yr
34 oscillation as a signal of core-origin.

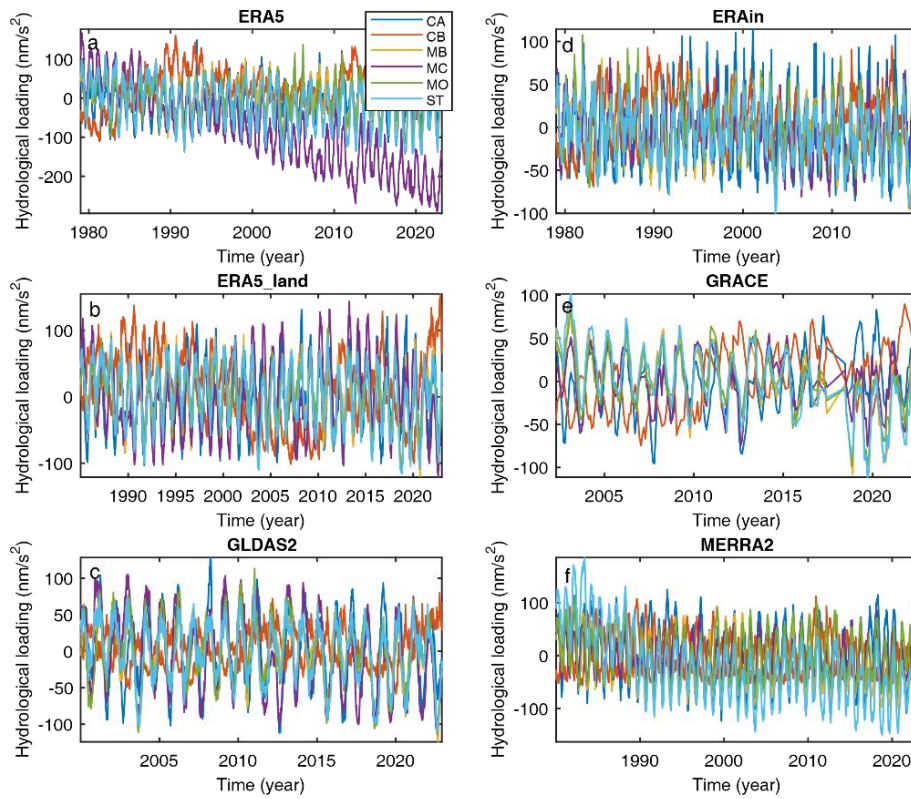
35 **Response:** We appreciate your comments and the references that you supplied. Here the main question
36 of controversy is whether or not the hydrological loading contains the 5.9-year oscillation (SYO)
37 (alternatively, whether or not the hydrological effects contribute to the observed SYO gravity change).
38 In addition, you brought to my attention that previous research found that the other climatic time series
39 indicate a 6-year oscillation. In response to these two issues, the following will give detailed
40 verifications using publicly accessible data from four perspectives.

41 42 **(1) Verification using hydrological loading models at IGEST sites**

43 We collected the hydrological loading data at six SG stations selected in this study from 6 different
44 global hydrological models (Fig. 1), including ERA5, ERAIn, ERA5-land, GRACE, GLDAS2, and
45 MERRA2, provided by the EOST Loading Service (http://loading.u-strasbg.fr/sg_hydro.php). We use
46 Fourier and Morlet wavelet spectra to verify whether the modeled hydrological loading data contain
47 the SYO signals.

48
49 Fig. 2 shows the Fourier amplitude spectra of the modeled hydrological time series at six SG stations.
50 The spectral analysis findings indicate that none of the hydrological models exhibit any noteworthy
51 peaks that align precisely with the SYO frequency ($1/5.9\text{years}=0.1695\text{cpy}$, as denoted by the horizontal
52 red lines). Nonetheless, there exist proximate peaks within the period band around 5.9 years, such as
53 the peaks of ~ 5.4 years at the CB station and ~ 6.4 years at the CA station. Moreover, we plot the Morlet
54 wavelet spectra of the hydrological data obtained from the ERA5 model and GRACE iterated global
55 mascons in Figs. 3 and 4, respectively. The ERA5 hydrological data at all SG stations exhibit a
56 deficiency in power at the ~ 5.9 -year intradecadal variability. The GRACE hydrologic data at the CB,
57 MO, MB, and ST stations exhibit some degree of power during certain time intervals. However, these
58 signals do not demonstrate significant and consistent SYO patterns in the studied time spans.

59

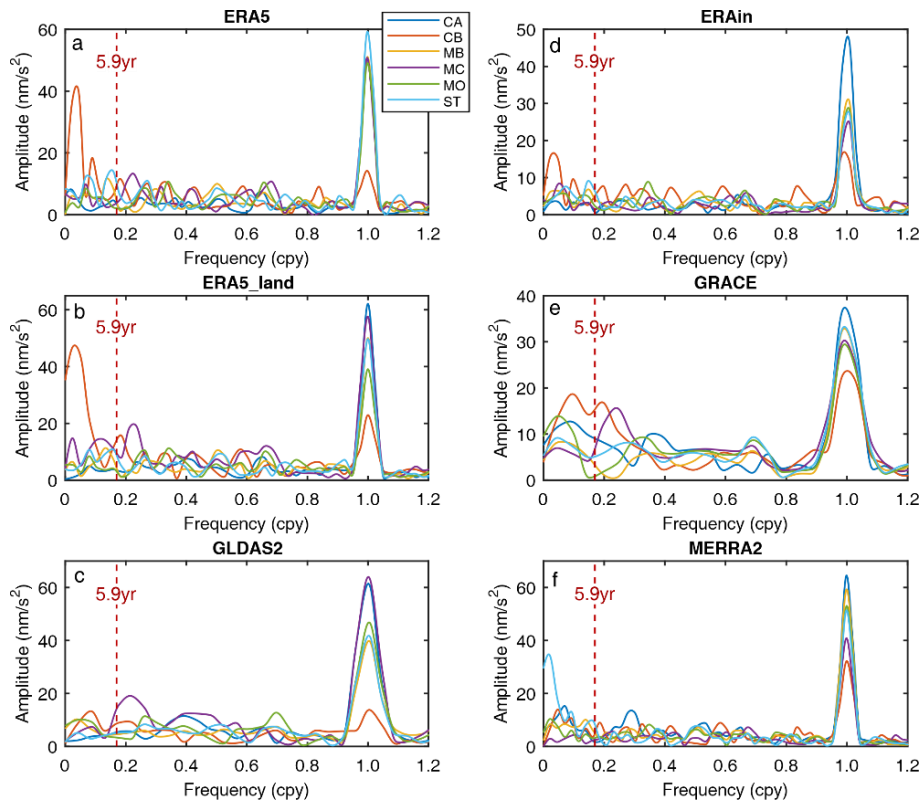


60

61 **Figure 1. Modeled hydrological loading data series at six SG stations: (a) ERA5, 1979-2023; (b)**

62 **ERAIn, 1979-2019; (c) ERA5-land, 1985-2023; (d) GRACE, 2002-2022; (e) GLDAS2, 2000-2022; (f)**

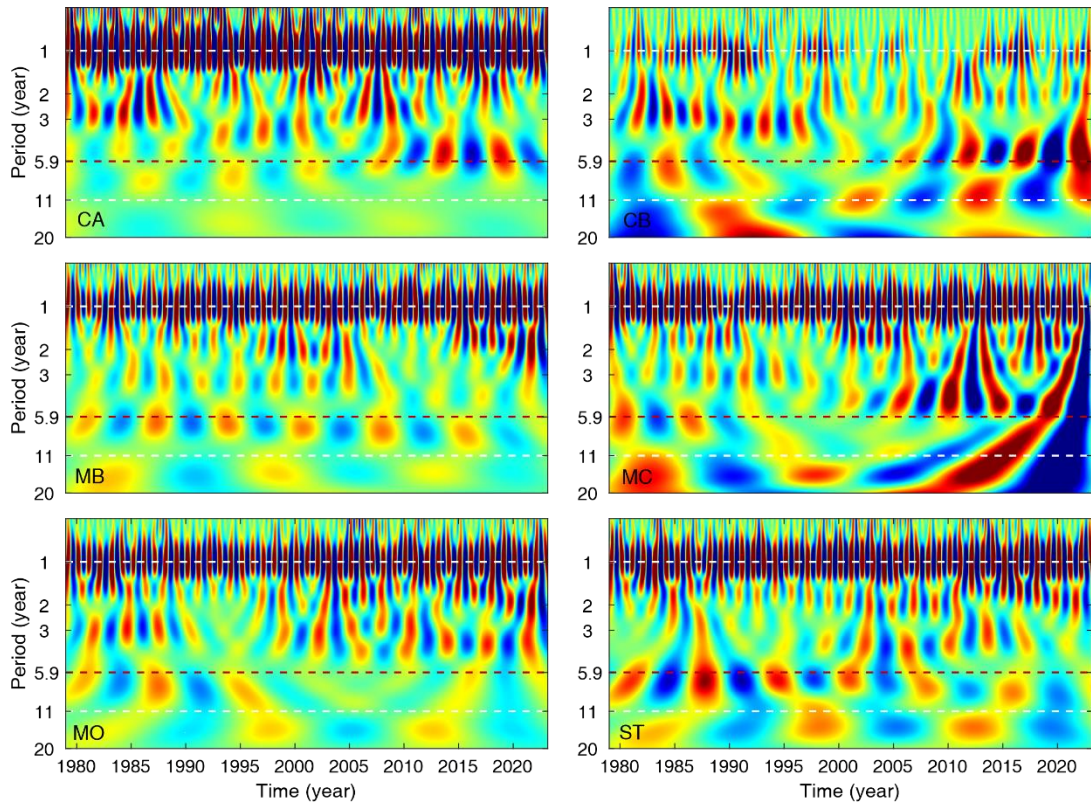
63 **MERRA2, 1980-2023.**



64

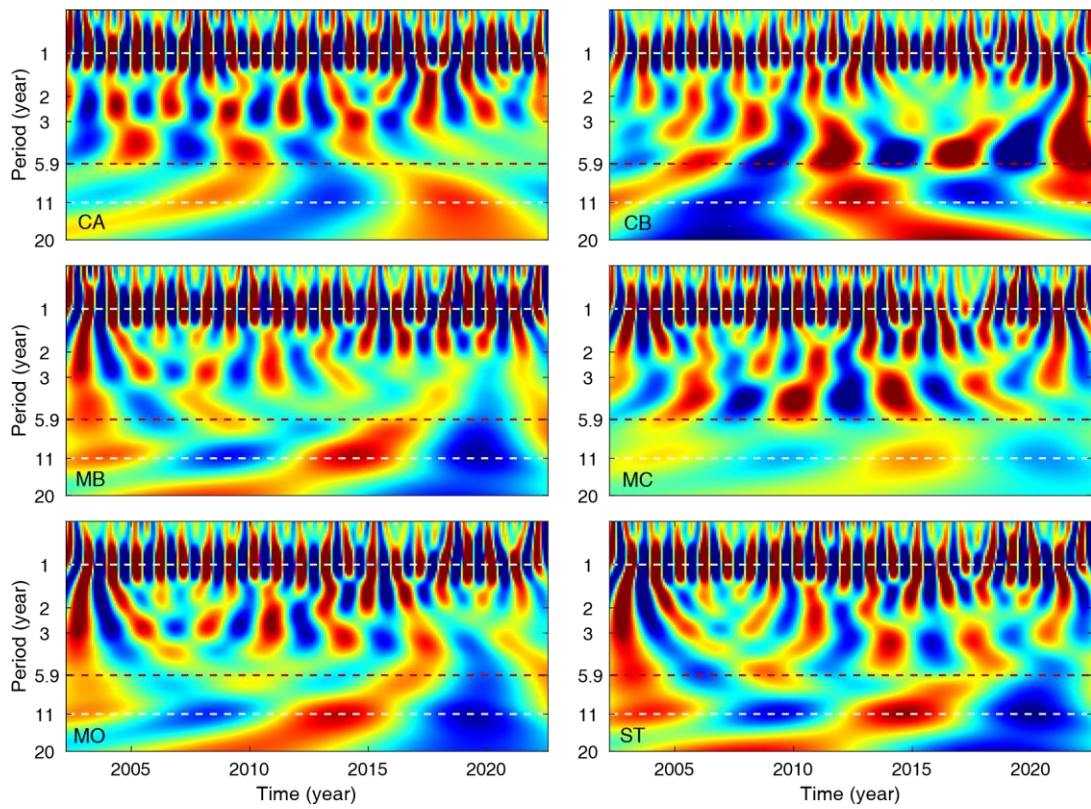
65 **Figure 2. Fourier amplitude spectra of the hydrological loading data series in Fig. 1. The vertical red**

66 **dashed lines denote the reference period 5.9 years of the SYO signal.**



67

68 **Figure 3.** Morlet wavelet spectra of the hydrological data series estimated from ERA5 model.



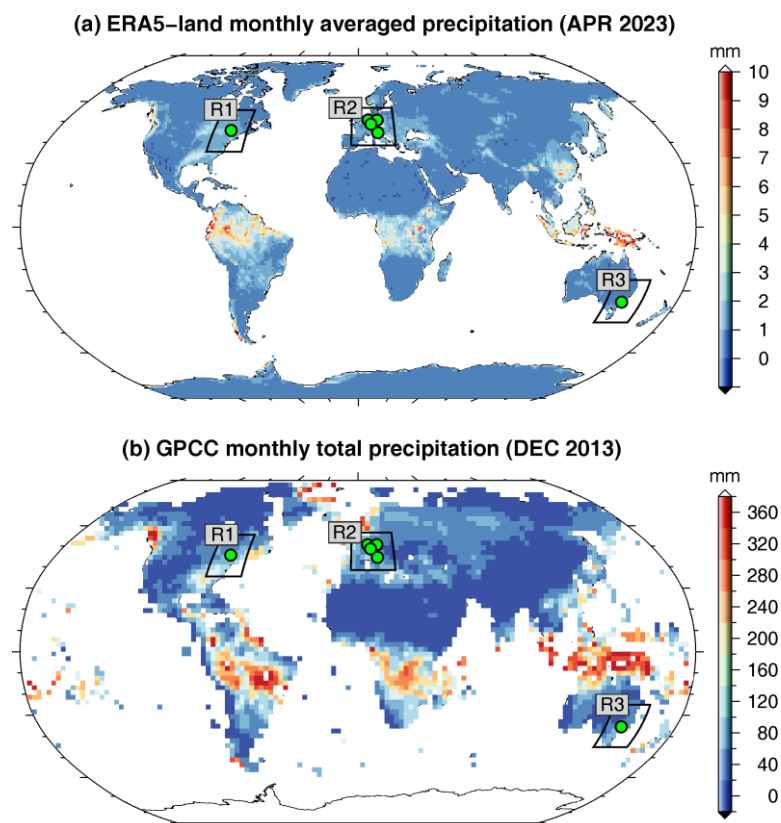
69

70 **Figure 4.** Morlet wavelet spectra of the hydrological data series estimated from GRACE iterated global
 71 mascons.

72 **(2) Verification using global gridded precipitation data**

73 According to Pfeffer et al. (2022, 2023), the 6-year oscillation could potentially originate from either
74 precipitation or terrestrial water storage (TWS). Pfeffer et al. (2023) applied a band-pass filter to isolate
75 the frequency band around the 6-year signal from the time series of precipitation or TWS anomalies,
76 derived from satellite gravity observations, in-situ and satellite-based precipitation records, and
77 predictions from global hydrological models. Here we employ the Fourier and wavelet spectra to
78 examine the monthly precipitation data series obtained from the ERA5-Land global gridded
79 precipitation model (<https://cds.climate.copernicus.eu/cdsapp#!/dataset/reanalysis-era5-land-monthly-means>) and GPCP
80 global gridded precipitation dataset (<https://psl.noaa.gov/data/gridded/data.gpcp.html>). With the exception of the entirety of the Earth's land surface, our attention is directed
81 towards specific regions (R1, R2, R3) that encompass the used SG stations in order to involve the
82 precipitation effects on both global and regional scales (see Fig. 5).
83

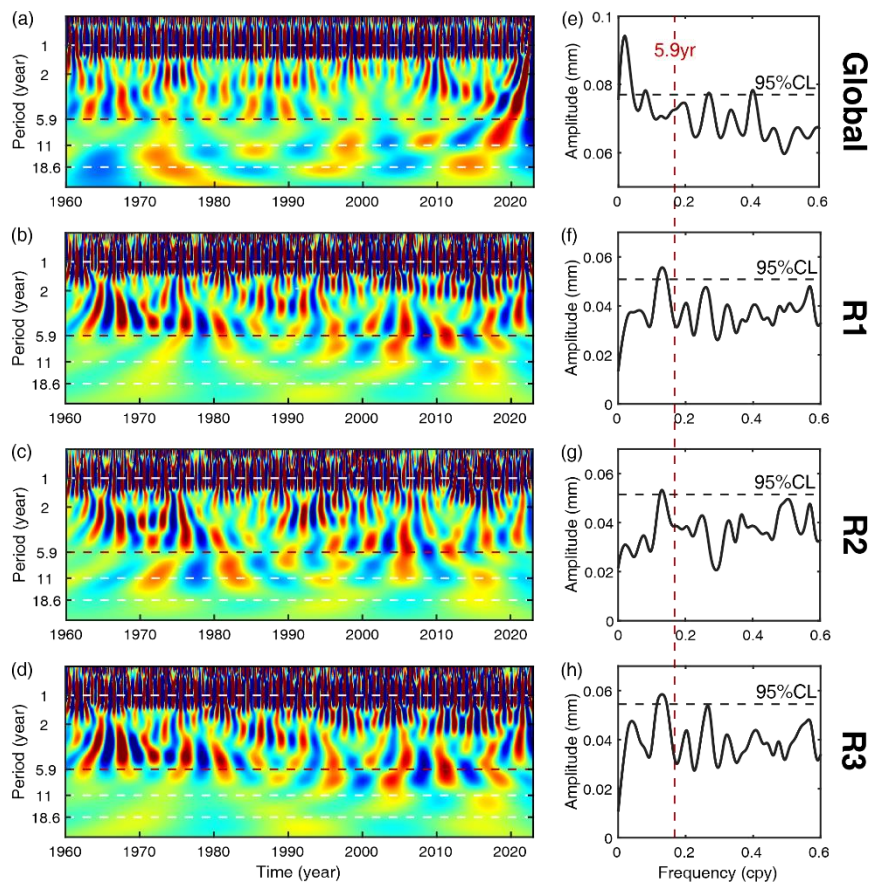
84



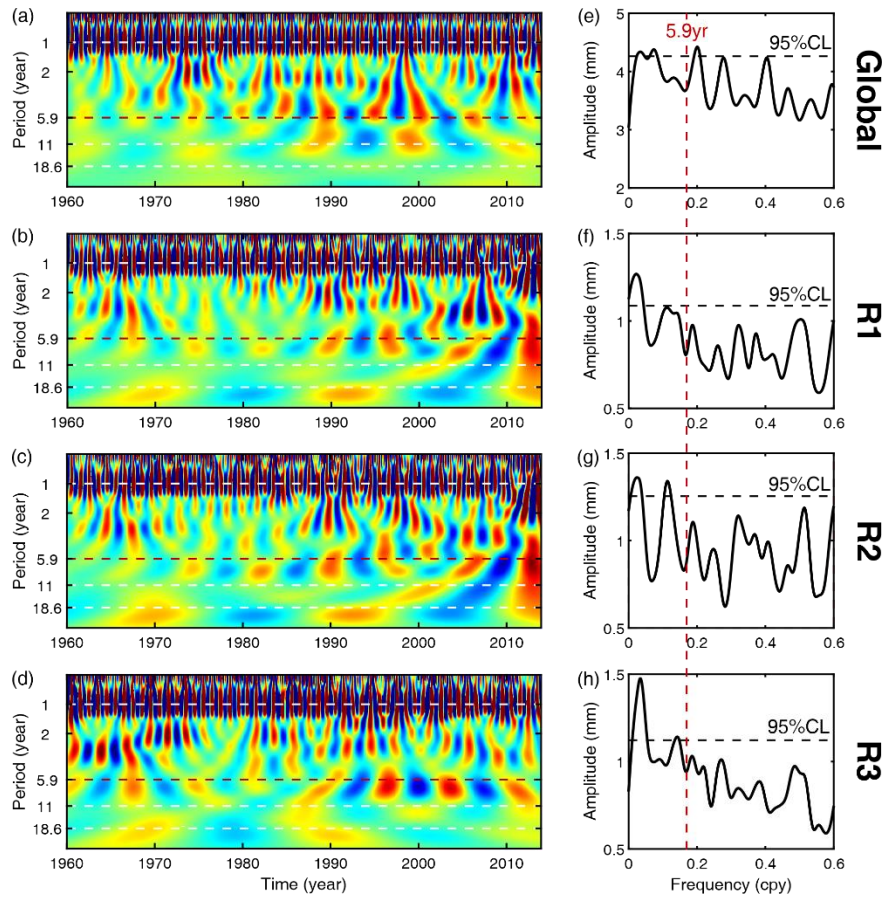
85

86 **Figure 5. Global gridded precipitation data:** (a) The ERA5-Land monthly averaged precipitation
87 model resampled at a $1^\circ \times 1^\circ$ grid, in Apr. 2023; (b) The GPCP monthly total precipitation observations
88 sampled at a $2.5^\circ \times 2.5^\circ$ grid, in Dec. 2013. The black frames labeled by R1, R2, and R3 indicate the
89 regions covering the used SG stations, respectively CA, MB/MC/MO/ST, CB (green circles).

90 In Fig. 6 the Fourier and wavelet spectra of the ERA5-Land precipitation data in the global, R1, R2,
 91 and R3 regions indicate no oscillation signal at the 5.9-year period. Within the period band around 5.9
 92 years, a peak of approximately 5.0 years is observed, with a low signal-to-noise ratio (SNR) and the
 93 amplitude lower than the 95% confidence level (CL) in the frequency band under investigation (Fig.
 94 6e-h). It is worth noting that the wavelet spectra for the global region exhibit evident annual signal,
 95 11-year fluctuation, and 18.6-year lunar tide on annual-to-decadal timescales (Fig. 6a, e). In Fig. 7 an
 96 analogous examination is conducted for GPCCC precipitation observations based global station data.
 97 The Fourier spectra exhibit peaks of ~ 5.2 years in the vicinity of a 5.9-year period (Fig. 7e-h); however,
 98 these peaks do not manifest as consistent oscillatory signals in the wavelet spectra (Fig. 7a-d). Despite
 99 the presence of consistent power levels lasting ~ 5.9 years in narrow time intervals (Fig. 7a), we think
 100 that these occurrences may be attributed to errors in modeling or reanalysis.



101
 102 **Figure 6. ERA5-Land precipitation model:** (a-d) The Morlet wavelet spectra of the average series
 103 of the detrended precipitation data in the global, R1, R2, and R3 regions. (e-h) The mean Fourier
 104 amplitude spectra of the detrended precipitation data series in the global, R1, R2, and R3 regions. The
 105 precipitation time series span from Jan. 1960 to Apr. 2023. The horizontal and vertical red dashed lines
 106 denote the reference period 5.9 years of the SYO signal, and the horizontal black dashed lines in (e-h)
 107 show the 95% confidence level (CL).



108

109 **Figure 7. GPCCC precipitation observations:** (a-d) The Morlet wavelet spectra of the average series
 110 of the detrended precipitation data series in the global, R1, R2, and R3 regions. (e-h) The mean Fourier
 111 amplitude spectra of the detrended precipitation data series in the global, R1, R2, and R3 regions. The
 112 precipitation time series span from JAN 1960 to DEC 2013.

113

114 To sum up, we do not find any significant and consistent ~ 5.9 -year oscillation in the hydrological
 115 loading model data and global gridded precipitation data. From previous studies of Δ LOD,
 116 geomagnetic fields, and SLR, it has been observed that the SYO behaves a relatively stable fluctuation
 117 with (e.g., Liao and Greiner-Mai, 1999; Gillet et al., 2010; Ding & Chao, 2018, EPSL; Ding, 2019;
 118 Duan & Huang, 2020; Chao & Yu, 2021; Ding et al., 2021). Besides, the hydrology-excited LOD time
 119 series does not contain the ~ 5.9 -year signal and the overall influences of the hydrology on Δ LOD are
 120 very small, but the atmosphere-excited LOD time series contains a ~ 5 -year signal (Zotov et al., 2020;
 121 Ding et al., 2021). Based on the aforementioned verifications and analysis, we preliminarily consider
 122 that the hydrological loading does not contain the SYO signal. However, the accuracy of the used
 123 reanalysis models or datasets cannot be ascertained with certainty, thus further demonstration is
 124 required to determine whether there is a SYO signal in continental hydrology. The optimal and

125 persuasive approach entails showcasing in-situ surface observation data, such as precipitation, soil
126 water, and groundwater level.

127

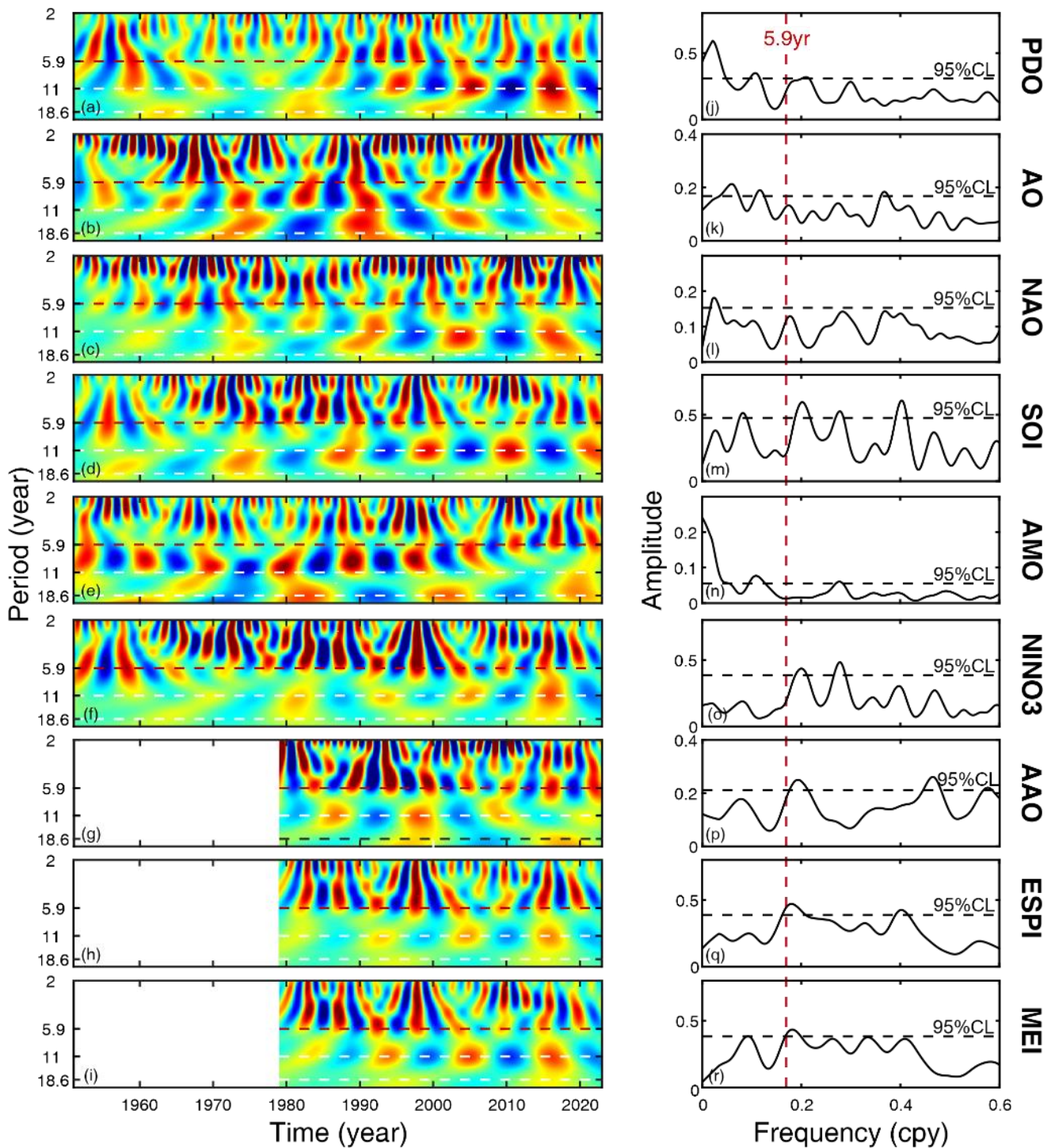
128 **(3) Verification using climate indices, GMST, and GMSL**

129 The research conducted by Moreira et al. (2019) and Pfeffer et al. (2023) is what we will be referring
130 to in the present verification. Moreira et al. (2019) focused on the interannual variabilities in global
131 mean sea level (GMSL) over 1993-2019, which were linked to various climate modes or indices.
132 Pfeffer et al. (2023) employed a bandpass filter to examine the time series of the global mean sea
133 temperature (GMST) and GMSL over 1993-2002. Here we collected more abundant climate indices
134 from NOAA Physical Sciences Laboratory (NOAA PSL, <https://psl.noaa.gov/data/climateindices/>),
135 and GMST and GMSL data series from various institutions or workgroups. The classical Fourier and
136 wavelet spectra are still employed to analyze the data to mitigate potential methodological errors.

137

138 Fig. 8 displays the Morlet wavelet and Fourier spectra of the monthly climate index series,
139 encompassing PDO, AO, NAO, SOI, AMO, NINO3, AAO, ESPI, and MEI, from 1951 to the present.
140 Just looking at the period band around 5.9 years in the Fourier spectra (Fig. 8j-r), it is evident that,
141 except for AMO, there are peaks of ~5-5.6 years with the amplitudes surpassing the 95% CLs for the
142 majority of climate modes. Upon further observing the wavelet spectra (Fig. 8a-i), no substantial or
143 stable oscillation signal with a period of ~5.9 years was detected. The 5.9-year periodicity continues
144 to exhibit a degree of power in narrow time intervals, particularly in relation to PDO, NINO3, ESPI
145 and MEI over 2000-2020. Additionally, the NAO over 1951-1990 and SOI over 1990-2010 also
146 demonstrate this periodicity. However, as previously stated, the wavelet spectra is still incapable of
147 resolving a stable oscillation of ~5.9 years. It can be seen that the classical Fourier spectrum, which is
148 restricted to frequency resolution, occasionally exhibits unreliable low-frequency signals, which may
149 arise from the superposition of near-periodic signals in different time spans. Hence, in order to acquire
150 precise information pertaining to a long-period signal, it is more efficacious to scrutinize its
151 instantaneous fluctuations.

152



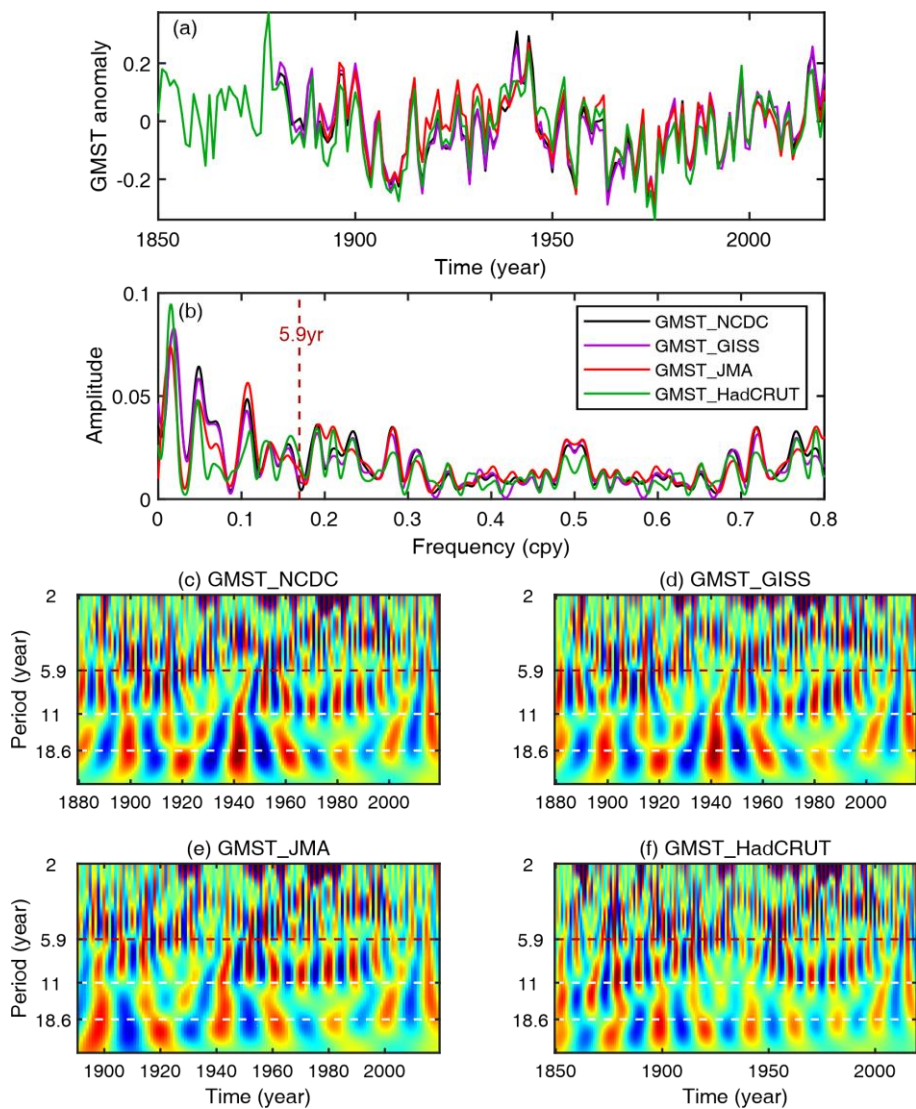
153

154 **Figure 8. NOAA Climate Indices:** The Morlet wavelet (left) and Fourier (right) spectra of the climate
 155 monthly index data series since 1951 to present. From top to bottom: Pacific Decadal Oscillation
 156 (PDO), Arctic Oscillation (AO), North Atlantic Oscillation (NAO), Southern Oscillation Index (SOI),
 157 Atlantic Multi-decadal Oscillation (AMO), Eastern Tropical Pacific SST (NINO3), Antarctic
 158 Oscillation (AAO), ENSO Precipitation Index (ESPI), and Multivariate ENSO Index (MEI).

159

160

161 Fig. 9 provides evident indication that there are no discernible peaks present at ~ 5.9 years in either the
 162 Fourier or Morlet wavelet spectra of the GMST anomaly data series. The horizontal white lines in the
 163 wavelet spectra show the resolved 18.6-year lunar tide signals (Fig. 9c-f), which are also identified in
 164 the Fourier spectra (Fig. 9b). The Fourier spectra also reveal the presence of notable peaks at the
 165 periods of ~ 10 years, which are in proximity to the 11-year oscillation albeit indiscernible in Fig. 9c-
 166 f. It is noteworthy that there exist peaks of ~ 6.3 years in the Fourier spectra, which align with the
 167 findings of Pfeffer et al. (2023) as depicted in their Fig. 8. However, these peaks have been confirmed
 168 to be fake signals in the wavelet spectra.



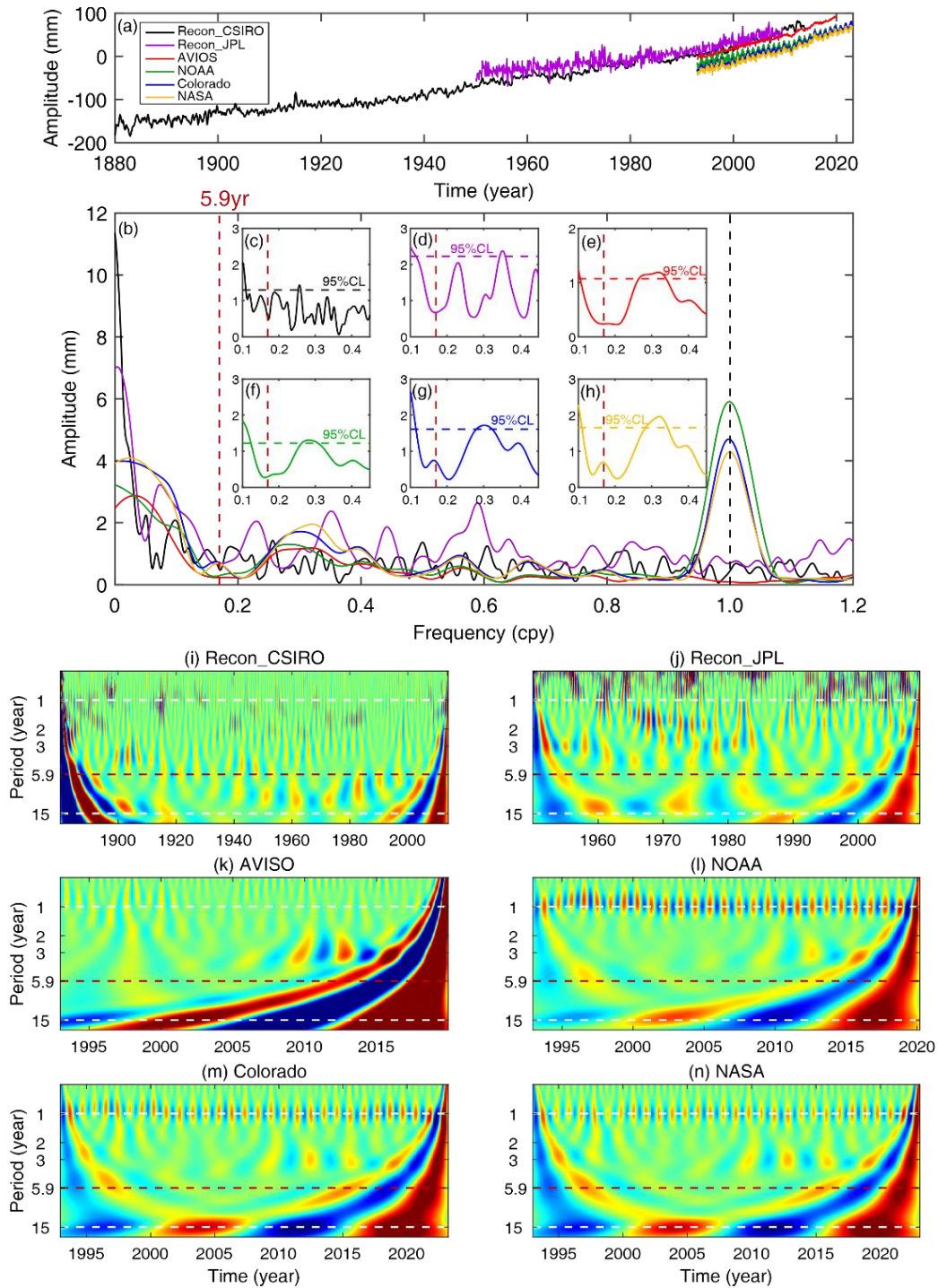
169
 170 **Figure 9. Global mean sea temperature (GMST):** The Fourier amplitude spectra (b) of the detrended
 171 annual GMST anomaly data series (a). Data source: GMST_NCDC (from NOAA/NCDC),
 172 GMST_GISS (from NASA/GISS), GMST_JMA (from Japan Meteorological Agency),
 173 GMST_HadCRUT5 (from Met Office Hadley Centre observations datasets).

174 Fig. 10 depicts the Fourier and Morlet wavelet spectra of the GMSL data series obtained from various
175 sources, including CSIRO, JPL, AVISO, NOAA, Colorado, and NASA. In the analyzed data sets,
176 specifically in the monthly reconstructed data from CSIRO and JPL and 10-day sampling data from
177 AVISO with seasonal signals removed, no discernible peaks were observed around the 5.9 years (Fig.
178 10c-e). In the time series from NOAA, Colorado, and NASA spanning from 1993 to present, with
179 seasonal signals retained, the very weak peaks around 5.9 years are detected in the Fourier spectra (Fig.
180 10f-h). These peaks are significantly lower than the 95% CLs. Furthermore, we do not find any
181 statistically significant signals exceeding the 95% CL around 6-7 years, especially 6.3 years, which
182 were exhibited by Moreira et al. (2019) and Pfeffer et al. (2023) in the power spectra density
183 periodogram.

184

185

186

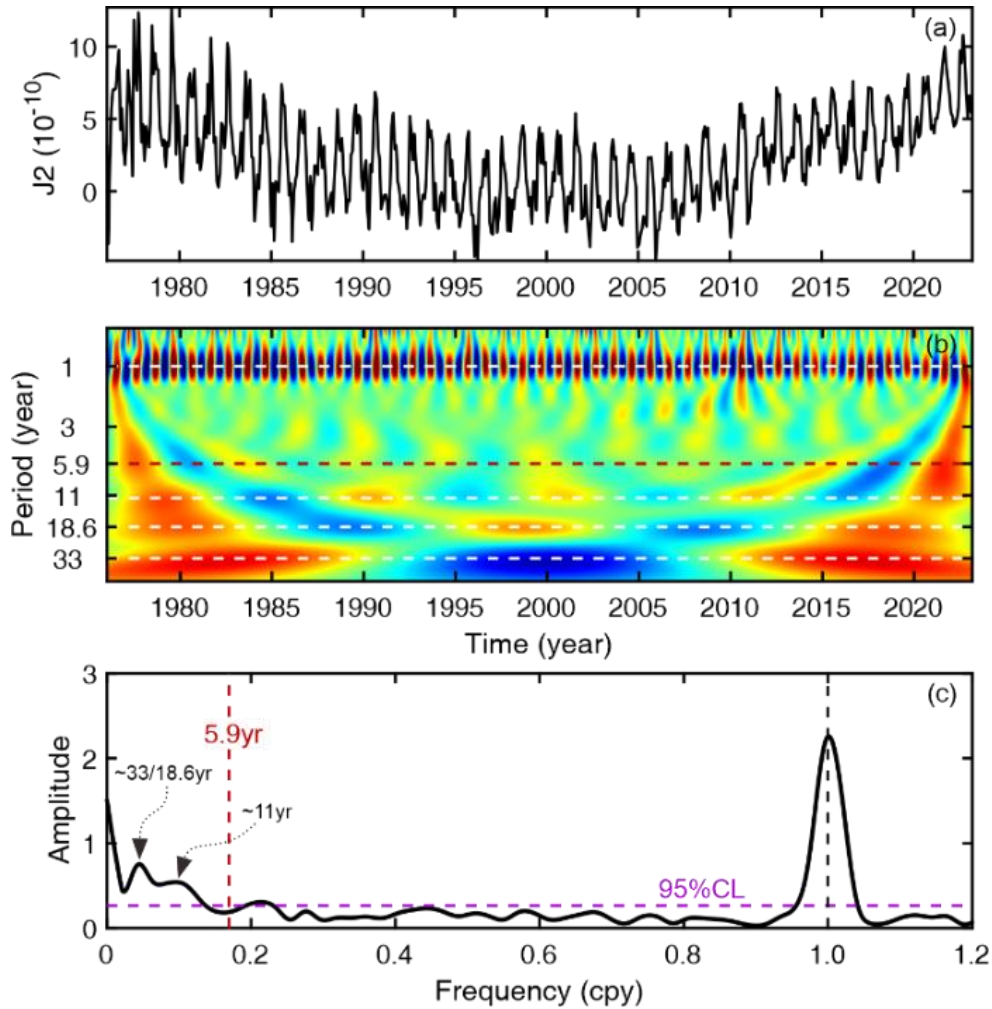


187

188 **Figure 10. Global mean sea levels (GMSL):** The Fourier (b-h) and Morlet wavelet (i-n) spectra of
 189 the GMSL data series (a). (c, i) Monthly reconstructed data from CSIRO (Common-wealth Scientific
 190 and Industrial Research Organization), 1880-2014; (d, j) Monthly reconstructed data from JPL (Jet
 191 Propulsion Laboratory), 1950-2009; (e, k) 10-day interval data from AVISO of CNSE (Centre National
 192 d'Etudes Spatiales), 1993-2020; (f, l) 10-day interval data from NOAA Climate.gov, 1993-2020; (g,
 193 m) Monthly data from Sea Level Research Group of University of Colorado, 1993-2023; (h, n)
 194 10-day interval data of TPJAOS v5.1 (Integrated Multi-Mission Ocean Altimeter Data) from the NASA Sea
 195 Level Change program, 1993-2023.

196 **(4) Verification using the oblateness ΔJ_2**

197 The terrestrial water storage variations can result in Earth's mass redistribution, potentially causing
198 the change of the Earth's shape (via private communication with Benjamin F. Chao). As per this
199 perspective, the J_2 variations (ΔJ_2), which serve as indicators of alterations in the oblateness of the
200 Earth, have the potential to reflect the global hydrological changes. Therefore, we use the Fourier and
201 wavelet spectra to analyze the ΔJ_2 time series spanning from 1975 to 2023
202 (https://filedrop.csr.utexas.edu/pub/slr/degree_2/). Fig. 11 demonstrates notable signals on
203 interannual-to-decadal timescales., i.e., the 18.6-year lunar tide and 11-year variation, which highly
204 coincide with the results of Chao et al. (2020). These signals are also found in the spectra analysis of
205 the ERA5-Land global precipitation model (see Fig. 6). Additionally, the Fourier spectrum reveals the
206 presence of a weak and spurious signal of a ~ 5 years period, which is consistent with the findings in
207 Fig. 6. This exemplary correlation serves to illustrate that the oblateness ΔJ_2 has the capacity to depict
208 certain overarching hydrological information on a global scale. The absence of a SYO signal in ΔJ_2
209 suggests a lower probability of the hydrological effects being the source of the SYO signal.



210

211 **Figure 11. ΔJ_2 :** The Morlet wavelet (b) and Fourier (c) spectra of the $\Delta J_2(t)$ data series (a) in 1975-
 212 2023. The oblateness J_2 is the Earth's lowest-degree gravitational component that measures the
 213 (normalized) difference between the polar and equatorial moments of inertia. The J_2 time series is
 214 concatenated from satellite laser ranging data (Cheng et al., 2004). The 18.6-year lunar tide, 11-year
 215 and 33-year fluctuations are prominent, but no appreciable presence of SYO is detected, ruling out a
 216 degree-2 order-0 mass change (a redistribution in the net meridional sense) for causing the SYO in
 217 hydrological effects (Ding et al., 2018, EPSL, Supplementary Materials).

218

219 Besides, the authors still employ the AR-z spectrum. This method has been used in many papers now,
 220 but the code is still not made publicly available. If it is so much better than the FFT, why you do not
 221 share it? This AR-z spectrum always displays additional peaks with respect to the FFT. How do you
 222 explain the additional peaks that are visible on Fig. 3 but not visible in FFT?

223 **Response:** Ding et al. (2018, JGR) have provided the test code of the AR-z spectrum in their Supporting
 224 Information (<https://agupubs.onlinelibrary.wiley.com/doi/10.1029/2018JB015890>). A Matlab code for

225 the AR-z spectrum, which includes a function code 'arz_spec.m' and a test code 'test.m' accompanied
226 by a detailed description, was recently made available to the public on ResearchGate
227 ([https://www.researchgate.net/publication/370231571_The_simply_Matlab_code_for_the_ARz_spec](https://www.researchgate.net/publication/370231571_The_simply_Matlab_code_for_the_ARz_spectrum)
228 [trum](#)). The methodology was executed and assessed by Hsu et al. (2021, JoG,
229 <https://doi.org/10.1007/s00190-021-01503-x>). The present study employed the stabilized AR-z
230 spectrum technique, which incorporated a Monte Carlo noise-assisted bootstrap scheme to yield more
231 robust spectral estimates for a single record. It should be noted that the shared codes and the one
232 verified by Hsu et al. (2021) are consistent as the core code to implement the AR-z method, without
233 considering the noise-adding process; whereas this noise-adding process for the stabilized AR-z
234 spectrum can be easily implemented (refer to Ding et al., 2018, JGR for details).

235
236 The AR-z spectrum exhibits several peaks with high SNRs, which are notably distinct from those
237 observed in the FFT spectrum. However, it is imperative to underscore that the power of the peaks in
238 the AR-z spectrum directly correlates with their stability rather than their actual amplitude. Please refer
239 to Ding et al. (2018, JGR)'s supporting information for the conclusion. In other words, the spectral
240 peak in the AR-z spectrum may appear strong even if the signal is weak, provided that it is relatively
241 stable. As seen in Fig. 3 of the manuscript, the atmospheric/oceanic/hydrological (AOH) signals in the
242 3-5 years frequency band are representative instances. The AR-z spectra of the CA, MO, and ST
243 stations exhibit insignificant spectral peaks, suggesting that the AOH signals are quite erratic during
244 the analysed time spans. This is also discernible in the wavelet spectra, as illustrated in Fig. 4 of the
245 manuscript.

246
247 P. 11, section 4.2: the argument of the ratio δ/h is not sufficient to propose an internal origin for the 6-
248 yr oscillation. This ratio for surface loading is also very different from the tidal one (see for instance
249 de Linage et al. 2007, doi: 10.1111/j.1365-246X.2007.03613.x and de Linage et al. 2009, doi:
250 10.1111/j.1365-246X.2007.03613.x, who have estimated this ratio for various loading and have shown
251 some variability). Local hydrology would also affect this ratio, particularly at underground stations
252 like Moxa, Membach, Strasbourg (e.g. Rosat et al. 2020, https://doi.org/10.1007/1345_2020_117).
253 This argument is hence not sufficient to justify your interpretation of the 6-yr oscillation as the
254 signature of an internal process.

255 **Response:** We first appreciate your valuable comments and providing us with significant references.
256 The degree-2 tidal Love numbers were exclusively taken into account to derive the ratio of δ/h , which
257 was determined to be approximately 1.9, while the surface loading ones were disregarded. This is an
258 important oversight in the manuscript.

259
260 The actions of surface gravity variations resulting from a surface load comprise of the load's direct
261 attraction and elastic deformation, and the latter also encompasses mass redistribution and free-air
262 effect (de Linage et al., 2007). According to de Linage et al. (2009), the average ratio for hydrological
263 loading (which includes soil moisture and snow) over the continents is $-0.87 \mu\text{Gal mm}^{-1}$, but this ratio
264 tends to increase as the size of river basins decreases; The atmospheric loading, assuming an inverted-
265 barometer response of the ocean, exhibits larger values for high latitudes, with a positive ratio of 0.49
266 $\mu\text{Gal mm}^{-1}$ (because the atmospheric masses are located above the measurement point); In the case of
267 ocean tidal loading, the mean ratio for diurnal tidal waves over the continents is $-0.26 \mu\text{Gal mm}^{-1}$. The
268 relationship between vertical deformation and surface gravity, as expressed by $\Delta g = -\frac{2g}{R} \frac{\delta}{h} \Delta V$,
269 allows for the approximate determinations of the ratios δ/h associated with the hydrological,
270 atmospheric, and ocean tidal loadings. Specifically, the ratios corresponding to these loadings are
271 approximately 2.84, 1.60, and 0.85, respectively. In contrast with our calculated values of 2.0 to 4.1,
272 the atmospheric and oceanic tidal loadings as the external sources of the SYO can be excluded, whereas
273 the hydrological loading's contribution to the SYO still needs intensive discussions. However, as
274 demonstrated in the above responses, we have confirmed that the hydrological loading has a negligible
275 impact on the surface gravity variation linked to the SYO.

276
277 Hence, it can be concluded that we can rule out that the SYO originates from external sources, but
278 attribute it to some internal dynamical processes, such as the MAC wave we suggested; the 6-year
279 related gravity changes, which may include core motions and some unknown 6-year changes due to
280 strong coupling interactions between the mantle and core. Namely, the 6-year related surface gravity
281 changes may be the result of a superposition of multiple internal motions in the Earth's coupling layers.
282 In fact, we have stated this opinion in the 2nd paragraph (lines 265-267) in Section 5, i.e., "we assume
283 that the Earth's core processes may also be coupled to the motions of other regions in the Earth, and

284 thus form secondary effects; And the magnitudes of which are not necessarily smaller than the direct
285 effects.” Except excluding the external loads, our conclusions are similar to the conclusions of
286 Cazenave et al. (2023) and Pfeffer et al. (2023), who suggested the SYO affects the Earth system as a
287 whole. These new discussions and references will be added to the revised manuscript.

288

289 Lines 270-272: the statement here is wrong. In Gillet et al. (2020) they used pressure Love numbers
290 exactly as in Greff-Lefftz et al. (2004). You can check the values for the Love numbers h in their
291 respective Table 1 and see that they are the same. The mistakes are in Fang et al. (1996) who have
292 considered the pressure flow as a surface load but they have ignored the deformation of the
293 equipotential surfaces in the core. They only considered the deformation of the mantle, while in Greff-
294 Lefftz et al. (2004) and in Gillet et al. (2020), they both considered the deformation of the mantle and
295 of the equipotential surfaces in the core. The Love numbers and surface deformation estimates by
296 Gillet et al. (2020) are hence correct.

297 **Response:** We have carefully re-read the articles by Gillet et al. (2020), Greff-Lefftz et al. (2004) and
298 Fang et al. (1996). Indeed, as you say, we have made a nonnegligible mistake. We will remove these
299 wrong discussions in the revised manuscript.

300

301 Technical corrections

302 Lines 51, 59, 64 etc... satellite laser ranging should be abbreviated as SLR not SRL

303 **Response:** Thank you for your correction for our clerical error, and we will revise the manuscript.

304

305 Line 73: the GGP project does not exist anymore, it has been replaced by the IGETS.

306 **Response:** We appreciate your corrections regarding the incorrect description in our manuscript, and
307 we will proceed to make the necessary revisions accordingly.

308

309 Lines 86-87: you say that you used level-2 products that mean that major disturbances have already
310 been corrected from the data. Else, please precise what you are referring to as “h2” corrections since
311 official IGETS products are called Level 1, Level 2 and Level 3 products.

312 **Response:** We must explain that the Code “h2” dataset, which is collected in the Level 2 data products,
313 includes hourly gravity and pressure data corrected for instrumental perturbations and ready for tidal

314 analysis (see Boy et al., 2020), was adopted for the used records (see Supplement Table S1 for the
315 detailed information). We will modify the manuscript to avoid unnecessary misunderstanding.

316

317 Line 154: in the processing of data, a tidal analysis was performed with ETERNA software to remove
318 tides. So why is there still the 18.6-yr tide? You did not include it in the groups of waves to be analyzed?
319 Why?

320 **Response:** We must declare that the long-period tide constituents, ranging from SA to MQM tides,
321 have been considered in our tidal analysis. However, as analyzed by many scholars, the harmonic
322 analysis results of long-period tides are not very ideal, i.e., exhibiting significant amplitude and phase
323 errors. This is attributed to that the time length is not enough for extracting precise information of long-
324 period tide through iterative least-squares. Therefore, we employed a simple approach by substituting
325 the long-period tide constituents with the ‘long’ wave, which operates within the frequency range of
326 0.004709-0.501369 cpd, and exhibits an amplitude and phase of 1.15000 and 0, respectively, as
327 recommended by Tsoft. This method includes the 18.6-year tide and also leaves the intradecadal
328 fluctuation unaffected.

329

330 Line 160: some spurious or unexplained peaks are visible in the AR-z spectrum (between annual and
331 QBO, and at 2.6-yr). Why you do not discuss them? Are they artefacts of the AR-z spectrum? How
332 confident are you on the AR-z spectral peaks? You should provide some confidence levels with this
333 method, since many spurious peaks seem to appear...

334 **Response:** The present study focuses on the analysis of interannual-to-decadal signals, as detailed in
335 Section 3. The signals within the frequency band of 1-2 years were not discussed, as they were
336 considered as background noise. The peaks in this frequency band were amplified to an observable
337 level because of the usage of an analytical continuation distinct from that employed in the interannual-
338 to-decadal band. Certain peaks may possess practical significance or could potentially arise from
339 background noise. Evidently, our unreasonable handling led to your misunderstanding. In the revised
340 manuscript, we will conduct a more meticulous analytic continuation of this frequency band to align
341 with the Fourier spectrum. Alternatively, we will employ a more straightforward method of low-pass
342 filtering during data preprocessing to eliminate the frequency band above 2 cpy and minimize the
343 influences of unidentified signals. Besides, it should be noted that during the implementation of non-

344 linear fitting for the recovery of the ~5.9-year oscillation, the frequency band of 1-2 years was not
345 considered due to its negligible impact on the retrieval process. Finally, we appreciate your reminder,
346 and the confidence levels for the AR-z spectra will be added in the revised manuscript.

347

348 **References**

349 Boy, J.-P., Barriot, J. P., Förste, C., Voigt, C., and Wziontek, H.: Achievements of the first 4 years of
350 the International Geodynamics and Earth Tide Service (IGETS) 2015-2019. In: Freymueller, J.
351 T., Sánchez, L. (eds) Beyond 100: The Next Century in Geodesy. International Association of
352 Geodesy Symposia, vol 152. Springer, Cham. https://doi.org/10.1007/1345_2020_94, 2020.

353 Cazenave, A., Pfeffer, J., Manda, M., and Dehant, V.: ESD Ideas: A 6-year oscillation in the whole
354 Earth system?, EGU sphere [preprint], <https://doi.org/10.5194/egusphere-2023-312>, 2023.

355 Chao, B. F. and Yu, Y.: Variation of the equatorial moments of inertia associated with a 6-year
356 westward rotary motion in the Earth, Earth Planet. Sci. Lett., 542, 116316,
357 <https://doi.org/10.1016/j.epsl.2020.116316>, 2020.

358 Chao, B. F., Yu, Y., and Chung, C. H.: Variation of Earth's oblateness J_2 on interannual-to-decadal
359 timescales, J. Geophys. Res. Solid Earth, 12, e2020JB019421,
360 <https://doi.org/10.1029/2020JB019421>, 2020.

361 Cheng, M. K. and Tapley, B. D.: Variations in the Earth's oblateness during the past 28 years, J.
362 Geophys. Res., 109, B09402, <https://doi.org/10.1029/2004JB003028>, 2004.

363 Ding, H.: Attenuation and excitation of the ~6-year oscillation in the length-of-day variation, Earth
364 Planet. Sci. Lett., 507, 131-139, <https://doi.org/10.1016/j.epsl.2018.12.003>, 2019.

365 Ding, H., An, Y., and Shen, W.: New evidence for the fluctuation characteristics of intradecadal
366 periodic signals in length-of-day variation, J. Geophys. Res. Solid Earth, 126, e2020JB020990,
367 <https://doi.org/10.1029/2020JB020990>, 2021.

368 Ding, H. and Chao, B. F.: A 6-year westward rotary motion in the Earth: Detection and possible
369 MICG coupling mechanism, Earth Planet. Sci. Lett., 295, 50-55,
370 <https://doi.org/10.1016/j.epsl.2018.05.009>, 2018.

371 Ding, H. and Chao, B. F.: Application of stabilized AR - z spectrum in harmonic analysis for
372 geophysics, J. Geophys. Res. Solid Earth, 123, 8249-8259,
373 <https://doi.org/10.1029/2018JB015890>, 2018.

374 Duan, P. S., and Huang, C. L.: Intradecadal variations in length of day and their correspondence with
375 geomagnetic jerks, *Nat. Commun.*, 11(1), 2273, <https://doi.org/10.1038/s41467-020-16109-8>,
376 2020.

377 Gillet, N., Jault, D., Canet, E., and Fournier, A.: Fast torsional waves and strong magnetic field
378 within the Earth's core, *Nature*, 465(7294), 74, <https://doi.org/10.1038/nature09010>, 2010.

379 Hsu, C. C., Duan, P. S., Xu, X. Q., Zhou, Y. H., and Huang, C. L.: On the ~7 year periodic signal in
380 length of day from a frequency domain stepwise regression method, *J. Geod.*, 95, 1-15,
381 <https://doi.org/10.1007/s00190-021-01503-x>, 2021.

382 Liao, D. C. and Greiner-Mai, H.: A new Δ LOD series in monthly intervals (1892.0-1997.0) and its
383 comparison with other geophysical results, *J. Geod.*, 73, 466-477,
384 <https://doi.org/10.1007/PL00004002>, 1999.

385 Moreira, L., Cazenave, A., and Palanisamy, H.: Influence of interannual variability in estimating the
386 rate and acceleration of present-day global mean sea level, *Global Planet. Change*, 199, 103450.
387 <https://doi.org/10.1016/j.gloplacha.2021.103450>, 2021.

388 Pfeffer, J., Cazenave, A., Blazquez, A., Decharme, B., Munier, S., and Barnoud, A.: Detection of
389 slow changes in terrestrial water storage with GRACE and GRACE-FO satellite gravity
390 missions, *EGUsphere [preprint]*, <https://doi.org/10.5194/egusphere-2022-1032>, 2022.

391 Pfeffer J., Cazenave A., Moreira L., Rosat S., Mandea M. and Dehant V.: A 6-year cycle in the Earth
392 system, *SSRN Electronic Journal*, <https://doi.org//10.2139/ssrn.4388237>, 2023.

393 de Linage, C., Hinderer, J., and Rogister, Y.: A search for the ratio between gravity variation and
394 vertical displacement due to a surface load, *Geophys. J. Inter.*, 171(3), 986-
395 994, <https://doi.org//10.1111/j.1365-246x.2007.03613.x>, 2007.

396 de Linage, C., Hinderer, J., and Boy, J. P.: Variability of the gravity-to-height ratio due to surface
397 loads, *Pure Appl. Geophys*, 166, 1217-1245, <https://doi.org/10.1007/s00024-004-0506-0>, 2009.

398 Zotov, L., Bizouard, C., Sidorenkov, N., Ustinov, A., and Ershova, T.: Multidecadal and 6-year
399 variations of LOD, *J. Phys.: Conf. Ser.*, 1705, 012002, [https://doi.org//10.1088/1742-
400 6596/1705/1/012002](https://doi.org//10.1088/1742-6596/1705/1/012002), 2020.